Gold catalyzed liquid phase oxidation of alcohol: the issue of selectivity

L. Prati,*[a] A. Villa,[a] C. E. Chan-Thaw,[a] R. Arrigo,[b] D. Wang[c] and D. S. Su[b]

Commercial carbon nanotubes (CNTs) and carbon nanofibers (CNFs) modified in various ways at the surface have been used as supports for gold nanoparticles (AuNPs) in order to study their influence on the activity/selectivity of catalysts in the aqueous oxidation of alcohol. Particularly oxidative treatment was used to introduce carboxylic functionalities, whereas subsequent treatment with NH_3 at different temperatures (473 K, 673 K and 873 K) produced N-containing groups leading to an enhancement of basic properties as the NH_3 treatment temperature was increased. The nature of the N-containing groups changed as the temperature increased, leading to an increase in the hydrophobicity of the support surface. Similar Au particle size and similar textural properties of the supports allowed the role of chemical surface groups in both the activity and the selectivity of the reaction of glycerol oxidation to be highlighted. An increase of basic functionalities produced a consistent increase in the activity of the catalyst, which was correlated to the promoting effect of the basic support in the alcoholate formation and the subsequent C–H bond cleavage. The selectivity towards primary oxidation products (C3 compounds) was the highest for the catalysts treated with NH_3 at 873 K, which presented the most hydrophobic surface. The same trend in the catalyst activity has been obtained in the aqueous benzyl alcohol base-free oxidation. As in the case of glycerol, the increasing of basicity and/or hydrophobicity increased the consecutive reactions.

Introduction

The success of gold as a catalyst for selective oxidation in the liquid phase is principally due to the peculiar characteristics of this metal compared to more classical Pd or Pt based catalysts when O_2 is used as the oxidant. In fact, it has been shown that a Au catalyst is less prone to deactivation in the presence of O_2 compared to Pd or Pt.[1–3] Moreover, gold catalysts show high selectivity towards the oxidation of primary alcohol with respect to secondary alcohol.[1,2] Since the first observation on ethylene glycol, a lot of papers have dealt with the application of gold catalysts to this important class of reaction, mainly with two aims. The first aim is to try to improve the activity and the second aim is to avoid parallel or consecutive reactions, thus enhancing the selectivity to the desired product. This latter aspect is very important from an application point of view and most recent studies focused on it. Moreover, the mechanistic understanding of the factors ruling selectivity become a priority task for optimizing catalyst design.

[a]Dipartimento di Chimica Inorganica Metallorganica e Analitica L. Malatesta, Università degli Studi di Milano, Via Venezian 21, 20133 Milano, Italy. E-mail: Laura.Prati@unimi.it
[b]Fritz Haber Institute of the Max Planck Society, Faradayweg 4-6, D-14195 Berlin, Germany
[c]Institut für Nanotechnologie, Forschungszentrum Karlsruhe in der Helmholtz-Gemeinschaft, Hermann-von-Helmholtz-Platz 1, 76344 Eggenstein-Leopoldshafen, Germany

One of the most studied substrates is benzyl alcohol, which can be selectively oxidized to benzaldehyde. Dehydrogenation on gold-supported nanoparticles to produce aldehyde can be competitive with the disproportionation of benzyl alcohol to benzaldehyde and toluene,[4] but dehydrogenation prevails when small gold nanoparticles (< 4 nm) are present. This is due to the increasing of the unsaturated coordination sites, which promotes the β C–H bond cleavage, which represents the rate determining step. This trend was confirmed also by periodic density functional theory (DFT) calculations[5] addressing the higher activity of small nanoparticles to the roughness of the surface. High selectivity to benzaldehyde (> 99%) has been reported depending on reaction conditions, *i.e.* solvent, temperature, but principally on the support employed (MgO and hydrotalcite).[4] The main by-products are represented by benzoic acid, benzyl benzoate (from consecutive reactions) or toluene and benzene (from parallel reactions). The selectivity of the reaction can be strongly affected by the presence of a base, whose function is still under investigation. It is believed that the base can cleave the O–H bond of the alcohol to form an alkoxide intermediate.[6] In this process, the role of the support (especially at the interface with the Au nanoparticles) and also the role of coadsorbed oxygen atoms on Au surface could be relevant.[4,7]

Glycerol represents another well-studied substrate, in view of its importance as a cheap material derived from biomass, on which a new chemical platform can be based.[8,9] Glycerol presents some fundamental differences compared to benzyl alcohol: the non-activating nature of the OH groups ($pK_a = 14$), the presence of primary beside secondary OH groups and the chelating nature (also of the oxidation products), which can strongly affect the catalyst life by providing irreversible adsorption and/or enhancing the leaching of metal. Moreover, another important difference lies in the aqueous solubility and the cheap availability of glycerol only in aqueous solution. Therefore, all the catalytic tests should be carried out in water instead of in organic solvent (toluene, xylene, cyclohexane) or solventless, as in the case of benzyl alcohol.

Since the first studies on glycerol oxidation,[1,2] it appeared evident that basic conditions enhanced both activity and selectivity positively. In fact, the presence of a base enhanced the reaction rate by facilitating the alkoxide formation[10,11] and by favoring
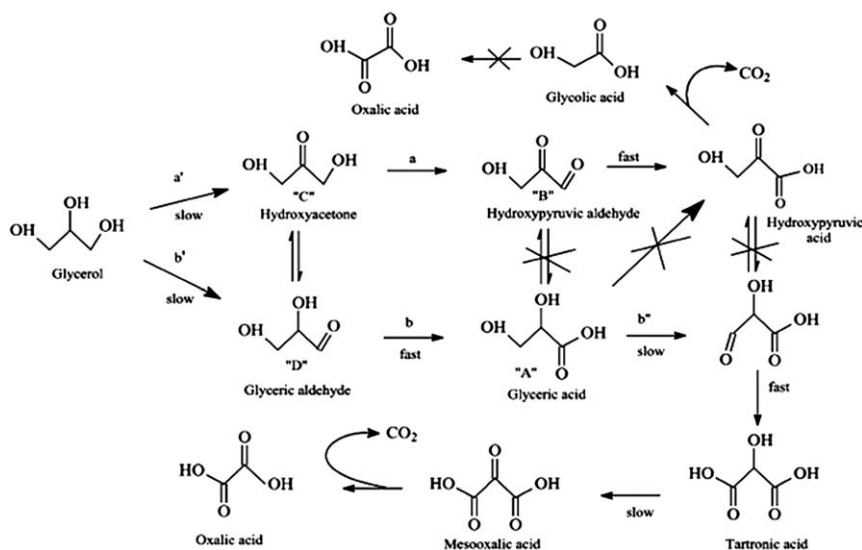
Scheme 1 Reaction scheme for glycerol oxidation under basic conditions.

the desorption of the highly-chelating hydroxyacid, thus decreasing irreversible adsorption on metal active sites.[12] In addition, basic conditions also have a beneficial effect on the selectivity towards the primary alcohol oxidation products (*i.e.* glycerate) (Scheme 1) through keto-enolic equilibrium and through accelerating the decomposition rate of H_2O_2 formed during the reaction, which has been recognized as responsible for the majority of the C–C bond cleavage products (*i.e.* glycolate, oxalate, formate).[10,13]

More recently, efforts in oxidizing glycerol in a base-free medium revealed the specific role of the support, but also showed evidence of the limitation in using monometallic gold based catalysts.[14] In fact, even under stronger conditions (373 K) than those used when the base was present (323–333 K), the reaction rates were very low and only the addition of a second metal (typically Pt) yielded a discrete reaction rate. Selectivity appeared to be determined mainly by the support. According to the model suggested by Davis, on the basis of DFT calculations and labeling tests,[11] the role of the support becomes fundamental in the second elementary step of the reaction, *i.e.* the hydration of aldehyde to acetal with the subsequent formation of the corresponding carboxylic acid. Thus, in this study, we investigated the role of the support in the selective glycerol oxidation further, mainly focusing our attention on the selectivity of the process.

Experimental

Materials

The gold sponge, 99.9999% purity, was purchased from Fluka. Commercial CNFs PR24-PS from Applied Science (average diameter of 88 ± 30 nm and a specific surface area of 43 m^2g^{-1}) and CNTs Baytubes (average diameter of 10 ± 2 nm and a specific surface area of 288 m^2g^{-1}) from Bayer were employed. The functionalization of the CNFs and the CNTs was performed according to the procedure report in ref. 15. The oxygen-containing nanocarbons were obtained by treating the pristine support with HNO_3 according to the following procedure: a solution of CNTs in HNO_3 concentrate (20 g of CNT per liter of HNO_3) was kept at 373 K for 2 h under continuous stirring, then rinsed with distilled water, and finally dried at 343 K for several hours. N-containing CNFs were obtained from the pre-oxidized CNFs by thermal treatment (10 g for each batch) with NH_3 in the temperature range 473–873 K for 4 h. $NaBH_4$ of purity > 96% purchased from Fluka and polyvinylalcohol (PVA) (M 10,000) from Aldrich were used. NaOH of the highest purity available was also from Fluka. Gaseous oxygen from SIAD (99.99% pure) was used. Glycerol (87% wt solution), glyceric acid and all the intermediates were purchased from Fluka. Benzyl alcohol, benzaldehyde, toluene and all the intermediates were also from Fluka.

Catalyst preparation

a) PVA-protected gold sol preparation. Solid $NaAuCl_4 \cdot 2H_2O$ (0.043 mmol) and PVA (2% wt) solution (1.64 mL) were added to 130 mL H_2O. After 3 min, $NaBH_4$ (0.1 M) solution (1.3 mL) was added to the yellow solution under vigorous magnetic stirring. The ruby red Au(0) sol was formed immediately.[16]

b) Immobilization step. Within a few minutes of sol generation, the sol was immobilised by adding the support under vigorous stirring. The amount of support was calculated to have a final gold loading of 1% wt. After 2 h, the slurry was filtered and the catalyst washed thoroughly with distilled water; it was then used in the wet form. ICP analyses were performed on the filtrate using a Jobin Yvon JV24 to verify the gold loading on the support.

Catalyst characterisation

a)   Titration procedure. Potentiometric titration of the basic sites was carried out on the samples using a Mettler Toledo Titrator. Approximately 0.2 g of sample was suspended in 50 mL of KCl 10^{-3} M and then sonicated and equilibrated for several hours. Prior to each measurement, the suspension was continuously saturated with argon to eliminate the influence of CO_2, until the pH was constant. Volumetric standards of HCl (0.01M) or NaOH (0.10M) were used as titrant, starting from the initial pH of the CNFs suspension.

b)   Metal loading. The gold content for the sol prepared catalysts was checked by ICP analysis of the filtrate on a Jobin Yvon JY24. The water content was determined by drying a sample at 423 K in air for 5 h. A check of Au loading was also performed directly on the catalysts, confirming the quantitative adsorption of Au NPs of the sol. The samples were weighed and loaded into a home-made NaCl crucible, then annealed at 973 K for two hours in air to burn off the carbon support. The residue was then dissolved in 5 mL of freshly made aqua-regia (3 : 1 hydrochloric/nitric acid – Omnipure grade – EMD). The sample was diluted to 50 mL with deionized water. ICP Standards were prepared by serial dilution of an Alfa-Aesar Au ICP standard. The dissolved NaCl had no effect on the ICP data.

c)   Morphology and microstructure of the catalysts were characterized by TEM. The powder samples of the catalysts were ultrasonically dispersed in ethanol and mounted onto copper grids covered with carbon film. A Philips CM200 FEG electron microscope, operating at 200 kV and equipped with a Gatan Tridiem imaging filter, was used for TEM observation. EDX analysis was performed in the same microscope using a DX4 analyzer system (EDAX).

Oxidation experiments

The reactions were carried out in a thermostatted glass reactor (30 mL) provided with an electronically controlled magnetic stirrer connected to a large reservoir (5000 mL) containing oxygen at 300 kPa.

Glycerol oxidation: 0.3 M Glycerol solution, NaOH (NaOH/glycerol = 4 mol mol^{-1}) and the Au catalyst (glycerol/metal = 1000 mol mol^{-1}) were added (total volume 10 mL). The reactor was pressurised at 300 kPa of O_2 and thermostatted at 323 K. After an equilibration time of 5 min, the reaction was initiated by stirring and samples were taken every 15 min and analysed by HPLC on a Varian 9010 HPLC equipped with a Varian 9050 UV (210 nm) and a Waters R.I. detector in series. An Alltech OA-1000 column (300 mm × 6.5 mm) was used with aqueous H_3PO_4 0.1% wt/wt M (0.5 mL min^{-1}) as the eluent. Samples of the reaction mixture (0.5 mL) were diluted (5 mL) using the eluent. Products were assigned by comparison with authentic samples.

Base-free reactions were carried out under the same conditions except for the temperature, which was increased to 373 K and glycerol/metal ratio (500 mol mol^{-1})

Benzyl alcohol oxidation: 0.3 M benzyl alcohol and the catalyst (substrate/metal = 500 mol mol^{-1}) were mixed in distilled water (total volume 10 mL). The reactor was pressurized at the desired pressure of O_2 and thermostatted at 333 K. The reaction does not start during the heating to temperature, as verified by sampling when the reaction temperature was reached without stirring ($t = 0$). The reaction was initiated by stirring. After the end of reaction, the catalyst was filtered off and the product mixture was extracted with cyclohexane. Recoveries were always 98% ± 3 with this procedure. For the identification and analysis of the products, a GC-MS and GC (a Dani 86.10 HT Gas Chromatograph equipped with a capillary column, BP21 30m × 0.53mm, 0.5 µm Film, made by SGE) were used. Comparison with authentic samples was used. For the quantification of the reactant-products, the calibration method using an external standard was employed.

Test for hydrogen peroxide degradation

A 1 mM solution of H_2O_2 (15 mL) was stirred at the appropriate temperature under N_2 atmosphere. The pH of the solution was adjusted by adding H_2SO_4 6 M (pH2). The amount of the catalyst added was the same as in the glycerol oxidation (about 20–30 mg). Hydrogen peroxide was quantified time by time by permanganate titration. The following procedure has been used: a sample (5 mL) of the filtered reacting solution was titrated with a 0.01 N $KMnO_4$ solution at constant pH of 2.0 ± 0.1 (by adding concentrated H_2SO_4). The detection limit of H_2O_2 was 0.01 mM.

Results and discussion

The selectivity of the reaction, as discussed above, can be strongly affected by the presence of a base. However, a relationship between particle size and selectivity was found.[1,2] Larger gold particles (> 10 nm) were more selective towards C_3-oxidation products than smaller ones, which produced a relevant amount of C–C bond cleavage products. However, more recent studies revealed that selectivity could be ruled by a more complex platform of factors.[17–19] Particularly the textural and chemical properties of the supporting material appeared to be fundamental.[17] In fact, it was reported that selectivity in the glycerol oxidation of Au on $MgAl_2O_4$ is tuned by the Al/Mg ratio at the surface besides the particle size and the exposure of the metal. Therefore, for studying the pure support effect in more detail, any other differences such as particle size, surface area and porosity of the supporting materials should be avoided. The selection of the materials was thus performed, taking into account the surface area (as high as possible to increase the metal dispersion) and porosity (avoiding as much as possible micropores for diffusional problems). Moreover, a surface which is easy to modify should be considered. Carbon nanotubes (CNTs) appeared to be good candidates, as they show regular textural properties with surface groups which can be modified by chemical/physical treatments without damaging the overall structure.

Two different commercial samples were used as starting materials. The characterizations have been recently reported:[20] one from Bayer Material Science A.G. (Baytubes, Carbon Nanotubes CNT) and one from Pyrograf Products Inc. (PR24, Carbon Nanofiber CNF). The physical properties of these two materials are reported in Table 1. An oxidative treatment (HNO_3 65% wt, 2 h, 373 K) increased the functionalization on the outermost walls, but did not significantly affect either the grain shape and the size, or the structure. An important effect of the treatment was, in both cases, to remove residual amorphous carbon from the surface. This procedure is known to increase the presence of carboxylic acids.[20] The acidic site titration confirmed an increase of the amount of acidic groups (Table 1). A basic functionalization was carried out by the subsequent treatment with NH_3 at different temperatures, following the procedure reported elsewhere.[21] Table 2 reports the basic site titration data that show the increase of the basic groups with increasing post-treatment temperature (473 K–673 K–873 K). It should be noted that, even at the highest temperature (873 K), the overall structure of CNFs was maintained.[21]

Table 1 Physical data for CNTs and CNFs

	AS ($m^2\ g^{-1}$)	Micropore area ($m^2\ g^{-1}$)	diameter (nm)	pH	mol acid sites/g
CNT	288[a]	40[a]	10 ± 2	10	—
CNT ox	321[a]	38[a]	10 ± 2	4.35	2.6×10^{-3}
CNF	43[a]	0[a]	88 ± 30	6.5	—
CNF ox	37[a]	5[a]	88 ± 30	4.52	4.5×10^{-3}

[a] From ref. [20,21].

Table 2 Titration data for N-CNFs

Sample	mol basic sites/g	Generated pH
N-CNF 473 K	$4.5*10^{-4}$	8.0
N-CNF 673 K	$6*10^{-4}$	8.2
N-CNF 873 K	$1*10^{-3}$	8.5

Table 3 Au particle size on CNTs and CNFs

|	Au sol	Au/CNT pristine	Au/ CNT ox	Au/CNF pristine	Au/ CNF ox	Au/N CNF 473 K	Au/ N-CNF 673 K	Au/ N-CNF 873 K
Statistical median (nm)	2.45	4.61	3.83	3.80	3.65	3.15	3.11	2.94
Standard deviation σ	0.27	1.32	0.89	0.95	0.78	0.57	0.64	0.51

CNTs and CNFs presented different surface areas, but the contribution of micropores could be considered negligible in both cases (Table 1).

We prepared thus Au supported nanoparticles (AuNPs) on CNTs and CNFs through the sol immobilization technique which represents the most suitable method for obtaining similar particle size distribution, regardless of the supporting material employed.[16] The Au particle size distributions obtained are reported in Table 3. During the immobilisation step, we noticed an increase in the size of the nanoparticles, probably due to coalescence that increases with decreasing interaction strength between the AuNPs and the support surface. As preformed AuNPs are identically generated in all the cases, we can address the difference in diameter of supported AuNPs to the different surface chemical groups and in particular to their density. Indeed, we observed similar particle diameter for AuNPs immobilized on all the treated supports (about 3–4 nm) with a decreasing of the discrepancy between diameter in the sol and on the support (*i.e.* before and after the deposition) by increasing the functional group density.

The acidic groups, introduced by oxidative treatment, appeared less efficient in stabilizing the nanoparticle diameter than the basic groups. In fact Au/CNT ox and Au/CNF ox showed the most remarkable increase in the Au particle diameter (3.83 and 3.65 nm *vs.* 2.94 nm for a comparable density of functional groups – Table 3). Pristine CNTs and CNFs lead to poor metallic dispersion, probably also due to the presence of amorphous carbon, which preferentially adsorbs the AuNPs from the sol. Some representative TEM pictures for Au/CNF and Au/CNT are shown (Fig. 1 and 2), demonstrating the increase in metal dispersion obtained after functionalization.

Regarding the activity of the catalysts, there are a lot of examples in the literature confirming that the activity of the catalysts in the liquid phase is related to the surface exposure of the active sites that should increase by decreasing the particle size.[17,18] In the present case, the external functionalization of the support surface, the negligible presence of micropores and the methodology chosen for the deposition of the gold nanoparticles should avoid the limitation due to diffusion problems. We should thus expect a trend of activities which follows the particle sizes. However, looking at the reaction profiles (Fig. 3 and 4) it can be seen clearly that this expected trend was not followed. In fact, Au/CNT ox and Au/CNF ox, even showing a very similar particle size distribution (mean size 3.83 nm *vs.* 3.65 nm – Table 3), presented

TOFs of 742 h^{-1} and 186 h^{-1}, respectively (Table 4 – Fig. 3). Also, Au/N-CNF 473 K and Au/N-CNF 673 K with almost the same particle size (3.15 nm and 3.11 nm, respectively) showed TOFs of 112 and 597 h^{-1}, respectively (Table 4 – Fig. 4). This definitely supports the idea that the supporting material plays an active role in determining the rate of glycerol oxidation. This is in agreement with the
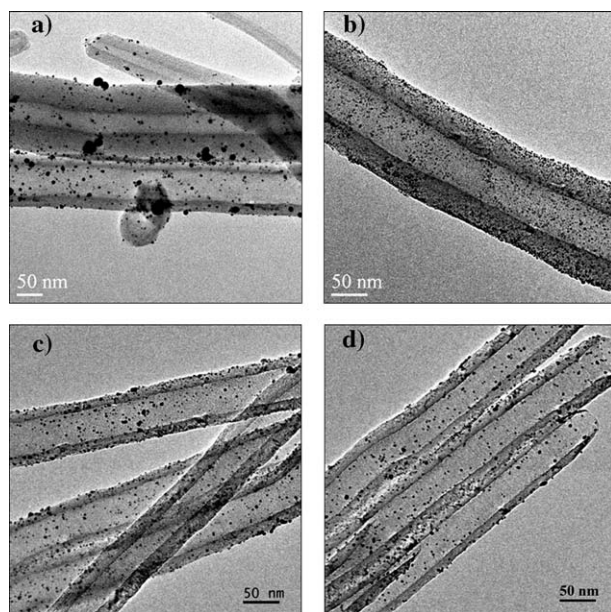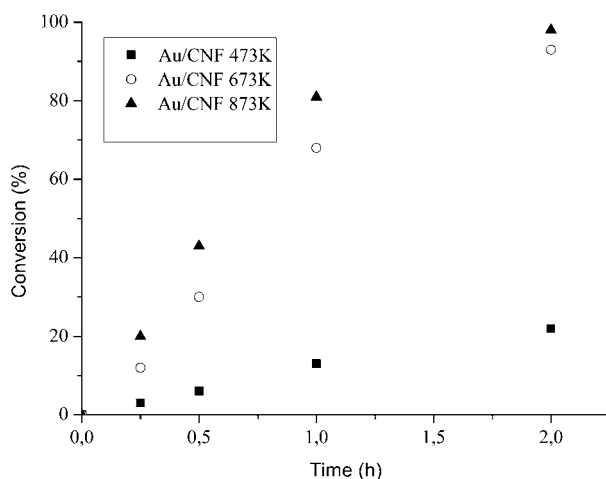

Fig. 1 TEM images of a) Au/CNF, b) Au/CNF ox, c) Au/CNT, d) Au/CNT ox.
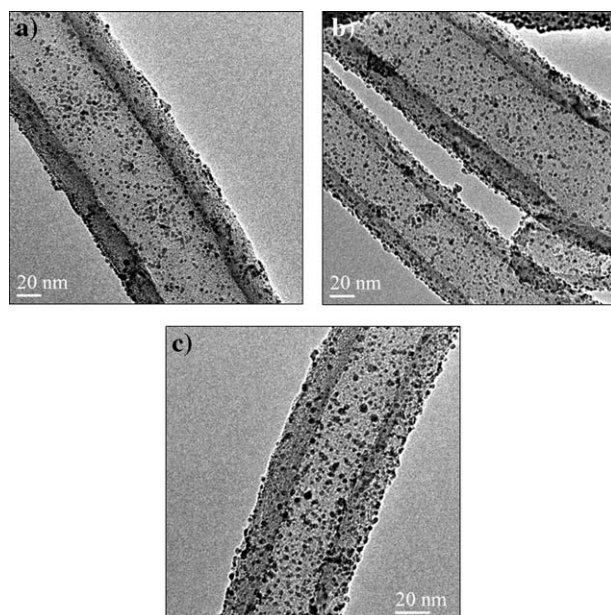
Fig. 2 TEM images of a) Au/N-CNF 473 K, b) Au/N-CNF 673 K, c) Au/N-CNF 873 K.
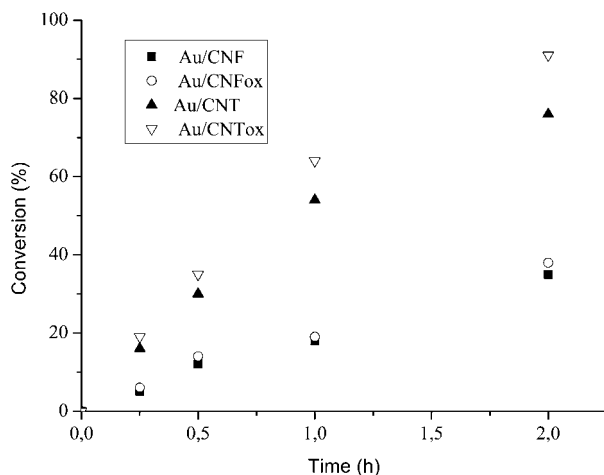
Fig. 3 Reaction profile for glycerol oxidation using Au/CNF, Au/CNT, Au/CNF ox and Au/CNT ox.

Fig. 4 Reaction profile for glycerol oxidation using Au/N-CNF 473 K, Au/N-CNF 673 K, Au/N-CNF 873 K.

mechanism depicted by Davis,[11] where it is the support which mediates the second and rate determining step of the reaction, *i.e.* the activation of the C–H bond of the ensuing alkoxide intermediate to form the aldehyde. Considering the NH_3 treated CNFs, it was thus not surprising that by increasing the basic site amount (Table 2) we observed an increasing of the catalyst activity in the same order (Fig. 4) even the huge difference between Au/N-CNF 473 K and Au/N-CNF 673 K was not fully justified by simply considering the increase of basic sites [Au/N-CNF 473 K (TOF 112 h^{-1}) < Au/N-CNF 673 K (TOF 597 h^{-1}) < Au/N-CNF 873 K (TOF 853 h^{-1})]. The positive effect on the catalytic performance in the liquid phase of NH_3 treatment has also been observed in the case of Pd supported NPs.[22] It should be noted, that the different functionalization temperature determined the presence of different surface chemical groups in the samples: at lower temperature (473 K) prevalent amide-like groups were observed, which were

transformed at higher temperature into pyridine-like groups.[21] In the sample treated at higher temperature (873 K), microcalorimetric measurements also revealed the presence of strong oxygen basic sites similar to those observed in hydrotalcite[23] and in γ-Al_2O_3,[24] along with a majority of weaker basic sites. The amination process produces a gradual increase of the hydrophobic character of the surface by increasing the temperature of the treatment.

Concerning the selectivity of the glycerol oxidation reaction (Scheme 1), Table 4 showed some unexpected results. On the one hand, using catalysts with similar Au particle size, we were expecting similar selectivity.[1,2] This did not occur, clearly indicating that some other factors influence the selectivity of the process. Pristine CNTs and CNFs showed different selectivity, CNTs being more selective toward C2 products (glycolate and oxalate) than CNFs (Table 4). In both cases, the oxidative treatment increased the selectivity towards C3 products (glycerate and tartronate) and did not alter the activity of the catalysts very much (Table 4 and Fig. 3). In the case of CNF, we observed a breakdown of selectivity for NH_3 treated samples, but only when the temperature of treatment was over 673 K, *i.e.* when the catalysts become more active. Indeed, selectivity did not change very much for Au/CNF, Au/CNF ox and Au/N-CNF 473 K, with 55–65% selectivity to glycerate, none to tartronate, 20–27% selectivity to glycolate and 10–16% selectivity to formate (Table 4— all the selectivities reported are at 90% conversion). On the contrary, in the case of Au/N-CNF 673 K and Au/N-CNF 873 K, a decrease of C2–C1 products (glycolate and formate) to 13% selectivity and 5–6% selectivity, respectively, was detected. Meanwhile an increase in C3 products (glycerate and tartronate) to 79–82% selectivity was observed (Table 4—all the selectivities reported are at 90% conversion). This behavior could be possibly explained by the surface properties related to the presence of different chemical groups. Accepting the H_2O_2 detected during the reaction as responsible for the C–C bond cleavage[10,13] and accepting that H_2O_2 derives from the O_2 reduction by H_2O adsorbed on the catalyst surface,[11] we could expect H_2O_2 formation to be related to the water adsorption capacity of the support, *i.e.* its hydrophilicity. The functionalization with HNO_3 and the subsequent treatment with NH_3 at different temperatures has been shown to increase the hydrophobicity of the surface progressively by increasing the temperature. Thus in our case, the increase of the basicity in Au/N-CNF 873 K should be expected to increase the activity by promoting the alcoholate formation and C–H bond cleavage, whereas the increase of surface hydrophobicity could lead to an higher selectivity to C3 by decreasing the H_2O_2 formation. However, during the tests, no significant differences in H_2O_2 concentration have been revealed. This was not surprising as the basic media could influence the degradation rate of the peroxide. Therefore, to better

Table 4 Glycerol oxidation with Au/CNTs and Au/CNFs under basic conditions[a]

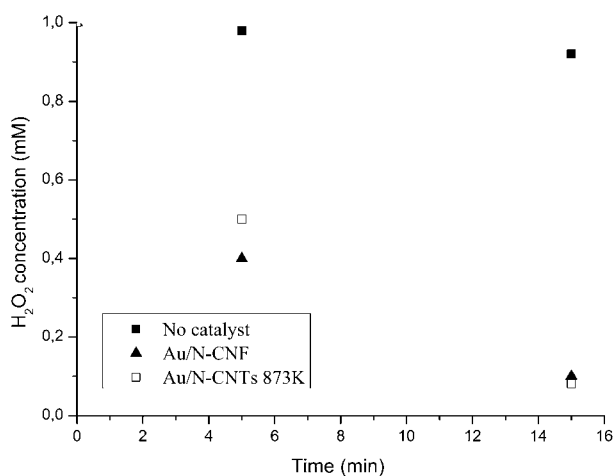| Catalyst	TOF[b] (h^{-1})	Selectivity[c]				
		Glycerate	Tartronate	Glycolate	Oxalate	Formate
Au/CNTs	648	26	7	14	53	<1
Au/CNT ox	742	59	11	17	13	<1
Au/CNF	182	55	1	27	0	16
Au/CNF ox	186	65	<1	20	0	10
Au/N-CNF 473 K	112	64	<1	22	0	12
Au/N-CNF 673 K	597	66	13	13	0	6
Au/N-CNF 873 K	853	68	14	13	0	5

[a] Reaction conditions: in water, glycerol/metal: 1000 mol mol^{-1}, $T = 323$ K, $pO_2 = 3$ atm., 4eq NaOH [b] TOF calculated at 30 min on the basis of total metal loaded [c] Selectivity at 90% conversion

Table 5 Base free oxidation of glycerol and H_2O_2 detected.[a]

| Catalyst | TOF[b] (h^{-1}) | Selectivity[c] | | | | | H_2O_2[d] mmol L^{-1} |
		Glycerate	Hydroxy pyruvic	Glycolate	Oxalate	Formate	
Au/CNF	0.5	41	17	12	0	30	1.5
Au/CNF ox	0.6	33	26	19	0	22	2.0
Au/N-CNF 473 K	1.3	30	20	22	3	23	2.0
Au/N-CNF 673 K	3.8	66	7	10	0	15	0.5
Au/N-CNF 873 K	4.7	62	8	13	-	16	0.3

[a] Reaction conditions: in water, glycerol/metal: 500 mol mol^{-1}, $T = 373$ K, $pO_2 = 3$ atm. [b] TOF calculated at 30 min on the basis of total metal loaded. [c] Selectivity at 20% conversion. [d] H_2O_2 from titration at isoconversion (20%).

clarify this point, we carried out some experiments under base-free conditions, as H_2O_2 is more stable at neutral-acidic pH. Tests under base-free conditions (373 K without any addition of base) showed a higher (even low) activity for Au/N-CNF 873 K, the most basic and hydrophobic catalyst. As under non-basic conditions we expected H_2O_2 to degrade more slowly than under basic conditions,[13] we can use the amount of C–C cleavage as a probe of H_2O_2 formation. Au/N-CNF 873 K, also under these conditions, produced C–C bond cleavage products (glycolate and formate) in a smaller amount than Au/CNF 473 K (Table 5). H_2O_2 quantification by titration confirmed a lesser concentration in the case of Au/N-CNF 873 K (0.3 mmol L^{-1} for Au/N-CNF 873 K vs 2.0 mmol L^{-1} for Au/CNFox – Table 5). Moreover blank experiments highlighted the same degradation rate for H_2O_2 in the presence of both catalysts (Fig. 5). These results seem to confirm our hypothesis that the hydrophobic nature of N-CNF 873 K contributed to the decrease in peroxide formation $i.e.$ an increase in C3-product selectivity. More accurate kinetic investigations are being carried out in order to confirm this finding.

Fig. 5 H_2O_2 degradation profile for Au/CNF and Au/CNF 873 K under acidic conditions (pH 2.5).
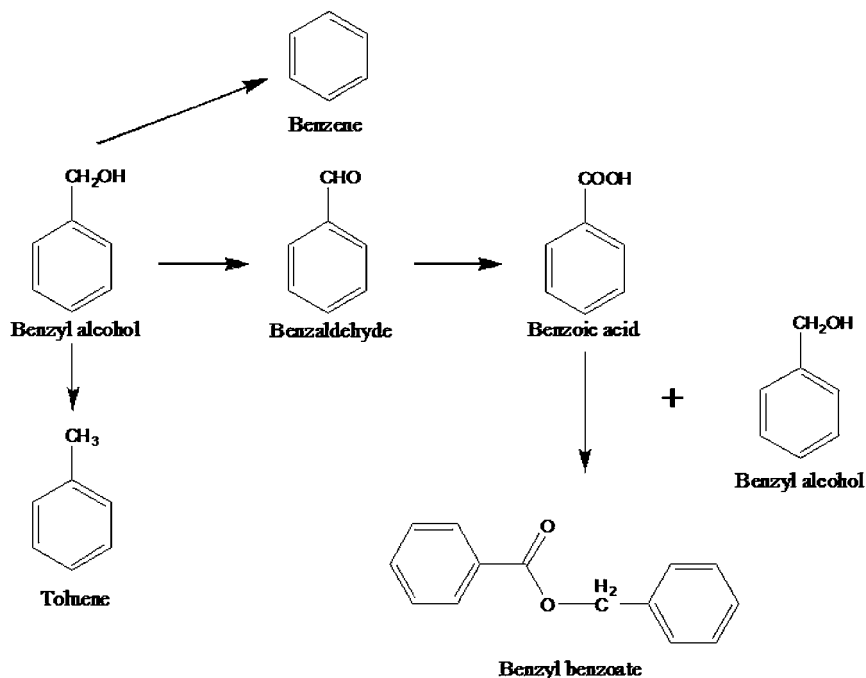
Table 6 Benzyl alcohol oxidation[a]

| Catalyst | TOF[b] (h^{-1}) | Selectivity[c] | | | |
		Benzaldehyde	Benzoic acid	Benzyl benzoate	Toluene
Au/CNF	7	92*	—	—	8
Au/N-CNF 473 K	65	93	2	—	5
Au/N-CNF 673 K	88	88	5	3	3
Au/N-CNF 873 K	102	85	8	3	3

[a] Reaction conditions: in water, alcohol/metal: 500/1, T = 333 K, pO_2 = 3 atm. [b] TOF calculated at 30 min on the basis of total metal loaded. [c] Selectivity at 90% conversion. *selectivity at 40% conversion.

Moreover, under base-free experimental conditions, it was shown that secondary alcohol can also be oxidized and hydroxypyruvic acid formed, highlighting for these two catalysts a different selectivity towards primary and secondary OH. Au/CNF 473 K appeared the most reactive and, considering that selectivity to glyceric acid is quite low, we could conclude that the oxidation of secondary alcohol is consecutive and most probably depends on a different adsorption mode.

Additional tests have also been performed using benzyl alcohol. The reaction was carried out in water without the addition of a base at 333 K. The increase of activity with the increase of basicity of the support could be expected, as well as the increase of benzoic acid, the formation of which is known to be favored by a basic environment[23] (Table 6). It should be noted, however, that, as in the case of glycerol, the consecutive reaction producing benzoic acid from benzaldehyde is favored by an increase in hydrophobicity of the support i.e. N-CNF 673 K and N-CNF 873 K

Scheme 2 Reaction scheme for benzyl alcohol oxidation.

(Scheme 2 – Table 6). We also observed a different distribution in the minor products of the reaction, namely benzyl benzoate and toluene. Benzyl benzoate could be considered formed through a consecutive reaction,[7] but the formation of toluene follows a different pathway, probably through dehydrogenation[5] (Scheme 2).

Conclusions

Alcohol oxidation in the liquid phase has been investigated, paying particular attention to the selectivity of the process and particularly to the role that the support can play. Reactions performed in water are of interest, because of the application to water soluble alcohol and particularly to glycerol, an important renewable feedstock. Commercially available CNTs and CNFs have been used as starting materials, because they did not present a relevant microporosity that could lead to diffusional limitation during liquid phase oxidation. Functionalization of CNTs and CNFs has been performed using the procedure set up by Arrigo et al.,[21] which produced fully characterized supports. Preformed gold sol has been immobilized on the supports, yielding Au catalysts with almost the same particle size, but showing different catalytic activity/selectivity as a function of the supporting material. In the glycerol selective oxidation it has been shown that the activity increased with the basicity of CNFs, whereas the selectivity appeared most related to the type of surface groups. Indeed, basic and hydrophobic surfaces enhanced the selectivity to C3 products, whereas more hydrophilic surfaces increased the C–C bond cleavage products. This behavior is possibly correlated to a higher concentration of native H_2O_2 detected in the presence of hydrophilic support.

Acknowledgements

References

1 S. Carrettin, P. McMorn, P. Johnston, K. Griffin, C. J. Kiely and G. J. Hutchings, *Phys. Chem. Chem. Phys.*, 2003, **5**, 1329.
2 F. Porta and L. Prati, *J. Catal.*, 2004, **224**, 397.
3 S. Demirel-Gulen, M. Lucas and P. Claus, *Catal. Today*, 2005, **102–103**, 166.
4 W. Fang, J. Chen, Q. Zhang, W. Deng and Y. Wang, *Chem.–Eur. J.*, 2011, **17**, 1247.
5 M. Boronat, A. Corma, F. Illas, J. Radilla, T. Ródenas and M. J. Sabater, *J. Catal.*, 2011, **278**, 50.
6 T. Ishida, M. Nagaoka, T. Akita and M. Haruta, *Chem.–Eur. J.*, 2008, **19**, 8456.
7 S. Meenakshisundaram, E. Nowicka, P. J. Miedziak, G. L. Brett, R. L. Jenkins, N. Dimitratos, S. H. Taylor, D. W. Knight, D. Bethell and G. J. Hutchings, *Faraday Discuss.*, 2010, **145**, 341.
8 C. H. Zhou, J. N. Beltramini, Y. X. Fan and G. Q. Lu, *Chem. Soc. Rev.*, 2008, **37**, 527.
9 A. Corma, S. Iborra and A. Velty, *Chem. Rev.*, 2007, **107**, 2411.
10 W. C. Ketchie, Y. Fang, M. S. Wong, M. Murayama and R. J. Davis, *J. Catal.*, 2007, **250**, 94–101.
11 B. N. Zope, D. D. Hibbits, M. Neurock and R. J. Davis, *Science*, 2010, **330**, 74.
12 N. Dimitratos, A. Villa, D. Wang, F. Porta, D. Su and L. Prati, *J. Catal.*, 2006, **244**, 113.
13 L. Prati, P. Spontoni and A. Gaiassi, *Top. Catal.*, 2009, **52**, 288.
14 A. Villa, G. M. Veith and L. Prati, *Angew. Chem., Int. Ed.*, 2010, **49**, 4499.
15 R. Arrigo, M. Hävecker, R. Schlögl and D. S. Su, *Chem. Commun.*, 2008, 4891.
16 L. Prati and G. Martra, *Gold Bull.*, 1999, **32**, 96.
17 A. Villa, A. Gaiassi, I. Rossetti, C. L. Bianchi, K. van Benthem, G. M. Veith and L. Prati, *J. Catal.*, 2010, **275**, 108.
18 A. Abad, A. Corma and H. Garcia, *Chem.–Eur. J.*, 2008, **14**, 212.
19 C. Lemire, R. Meyer, S. Shaikhutdinov and H.-J. Freund, *Angew. Chem., Int. Ed.*, 2004, **43**, 118.
20 J. P. Tessonnier, D. Rosenthal, T. W. Hansen, C. Hess, M. E. Schuster, R. Blume, F. Girgsdies, N. Pfaender, O. Timpe, D. S. Su and R. Schloegl, *Carbon*, 2009, **47**, 1779.

21 R. Arrigo, M. Haevecker, S. Wrabetz, R. Blume, M. Lerch, J. McGregor, E. P. J. Parrott, J. A. Zeitler, L. F. Gladden, A. Knop-Gericke, R. Schloegl and D. Su, *J. Am. Chem. Soc.*, 2010, **132**, 9616.

22 A. Villa, D. Wang, P. Spontoni, R. Arrigo, D. Su and L. Prati, *Catal. Today*, 2010, **157**, 89.

23 W. Winter, X. Xia, B. P. C Hereijgers, J. H Bitter, A. J. van Dillen, M. Muhler and K. P. de Jong, *J. Phys. Chem. B*, 2006, **110**(18), 9211.

24 J. Shen, R. D. Cortright, Y. Chen and J. A. Dumesic, *Catal. Lett.*, 1994, **26**(3–4), 247.